Understanding the Influence of Uncertainty and Noise on Spatial Decision Dynamics

Yirong Xiong (xiong.yirong.xyr@gmail.com)
1 Max Planck Institute for Brain Research, Max-von-Laue-Straße 4,
Frankfurt am Main, Hessen 60438, Germany

Vivek Hari Sridhar (vsridhar@ab.mpg.de)
2 Department of Biology,
University of Konstanz,
Konstanz 78464, Germany

3 Department for the Ecology of Animal Societies,
Max Planck Institute of Animal Behavior,
Konstanz 78467, Germany

4 Centre for the Advanced Study of Collective Behaviour,
University of Konstanz,
Konstanz 78464, Germany

5 Centre for Ecological Sciences,
Indian Institute of Science,
Bengaluru 560012, India

Abstract

In decision-making research, the speed-accuracy trade-off (SAT) is a pivotal concept, with prior studies demonstrating its optimization influenced by factors such as the system's internal noise and stimuli reliability (or uncertainty). Extending this understanding from conventional decision-making paradigms to spatial contexts, our study employs a ring attractor model to delve into the impact of external uncertainty and internal noise on the critical dynamics (or bifurcations) that accompany decision-making. Our findings reveal that increased internal noise delays the onset of this bifurcation, biasing decision accuracy over speed. Conversely, signal uncertainty exerts a U-shaped effect on the emergence of this bifurcation—moderate uncertainty accentuates speed, while low and high uncertainties favor accuracy. These insights contribute to our understanding of how SAT operates within spatial decision-making frameworks, particularly in complex environmental settings.

Keywords: Speed accuracy trade-off; Decision-making; Ring attractor; Noise

Introduction

Rapid and accurate decision-making among multiple spatial options is a fundamental challenge animals face in their daily life. Speed-accuracy trade-off (SAT) in these decisions is crucial, impacting survival in scenarios as varied as locating one of the trees as shelter at night or seeking paths to evade predators in the field.

Research on insects and zebrafishes has shown that during spatial navigation, the decision is usually made at a critical point (Sridhar et al., 2021). Initially, these animals might navigate towards an intermediate point between two choices. However, as the separation angle between these targets reaches a specific threshold, they commit to one target (Fig. 1A). This critical angle marks a dynamic shift within the system, enhancing sensitivity to quality differences between external stimuli (Amil & Verschure, 2021; Cocchi, Gollo, Zalesky, & Breakspear, 2017). Making a decision either before or after this critical point can lead to suboptimal outcomes: premature decisions may compromise accuracy, while delayed decisions could extend the overall journey unnecessarily. Consequently, this bifurcation is pivotal for SAT in spatial decision-making.

Research has found that both human and non-human animals can fine-tune their SAT strategies to optimize outcome under varying external and internal conditions (Bertucco, Bhanpuri, & Sanger, 2015; Manohar et al., 2015; Mendonça et al., 2020). When the stimuli reliability is low, decelerating the decision process allows more time for evidence accumulation; conversely, when immediate rewards are prioritized, accelerating the decision process can minimize the wait time for these rewards. However, in more complex spatial tasks, the modulation of SAT strategies remains less understood.

In our study, we use the ring-attractor model to examine how signal reliability (or external uncertainty) and system's internal noise impact SAT in two-choice spatial decision-making. We found that increased internal noise correlates with a larger decision-making angle, which extends the time required for evidence accumulation and consequently increases the travel distance. Conversely, external uncertainty exhibits a U-shaped relationship with this critical angle, indicating that with very small uncertainty, decision-making is

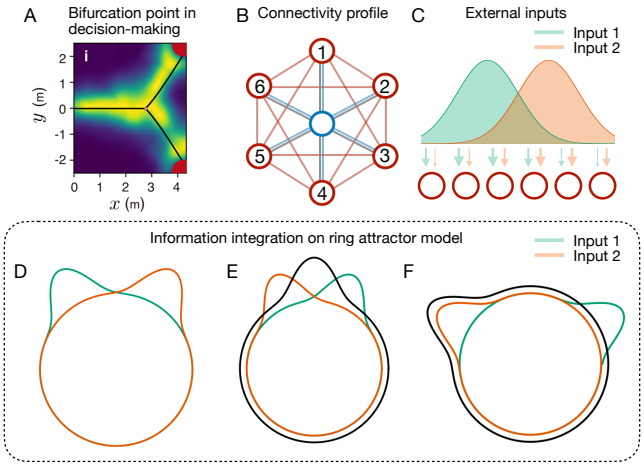

Figure 1: Trajectory density map of fruit flies navigating towards two identical targets (indicated by red dots), with the black line depicting a model fit to the trajectories (Sridhar et al., 2021). Initially, flies converge towards a target following an average direction; upon reaching a critical egocentric separation angle, they decisively turn towards one arbitrary target. **B)** Simplified ring attractor model. The simplified model consists of six excitatory neuron (red circles) and one inhibitory neuron (blue circle) (note there are 90 excitatory neurons in our model). All the neurons are self-connected and connected to each other. **C)** External inputs are two Gaussian function centered at different target directions. **D-F)** Signal integration of two input signals on ring attractor model. **(E)** For inputs with closely aligned directions, the model predicts an integrated signal that represents the average direction (black line). **(F)** For inputs with widely separated directions, the model (integrated signal) arbitrarily converges to one, or the other, input signal direction (black line).

slow due to the need for more extensive evidence accumulation with reliable but conflicting cues. These findings provide valuable insights into the interplay between noise, uncertainty, and SAT in decision-making, deepening our understanding of the underlying computational mechanisms involved in spatial choices.

Ring attractor model

The ring attractor model is a computational framework used in spatial sensory information integration (Kutschireiter, Basnak, Wilson, & Drugowitsch, 2023; Hulse & Jayaraman, 2020; Wilson, 2023). It is characterized by its consistent output—a Gaussian profile with a single peak—regardless of the variability in input signals (Wang & Zhang, 2020). The location of this integrated peak can be modulated by separation angle of inputs (θ): when θ is small, the peak will be at average of input peaks (Fig. 1E); when θ is big, the peak will bifurcate to align with one of the inputs (Fig. 1F). The ring attractor model has recently been employed to elucidate spatial decision-making at the behavioral level (Sridhar et al., 2021).

We took advantage of the information integration properties of ring attractor model to study the effect of noise in spatial decision making. Specifically, we constructed a Touretsky ring attractor model which comprises a single inhibitory neuron and 90 excitatory neurons, each with a unique preferred direction that collectively spans the entire navigational space (Sun, Mangan, & Yue, 2018; Touretzky, 2005).

Network Dynamics. We combined nonlinear activation function and integrate-and-fire model to simulate each neuron's activity (Brette & Gerstner, 2005). The average membrance potential of neuron m at time t, denoted as $u_m(t)$, evolves according to a differential equation that factors in time constants (τ_m), resting potentials ($u_{m\text{rest}}$), and leak resistances ($R_m = 1$) unique to each population of neurons (Eq. 1). For excitatory neurons, these parameters are set to $\tau = 0.05$, $u_{rest} = -1.5$, and for the inhibitory neuron $\tau = 0.005$, $u_{rest} = -7.5$. The nonlinear property is achieved by a ReLU function (Eq. 2) (Agarap, 2019).

$$\tau_m \frac{du_m}{dt} = f(-[u_m(t) - u_{m\text{rest}}] + R_m I_m(t)) \quad (1)$$

$$f(x) = max(0, x) \quad (2)$$

The input I_m to neuron m, comprises network-induced current (**internal input**) and target-induced currents (**external input**). The internal input is the weighted sum of all neurons' outputs and Gaussian **internal noise** $N(0, \sigma_n)$ (Eq. 3). The connectivity weight between excitatory neurons is set as a Gaussian function of the angular distance between their preferred directions, with standard deviation σ_w set to $\pi/3$ (Eq. 4, Fig. 1E).

$$I_m(t) = \sum_n^N w_{n\to m} u_n(t) + \xi N(0, \sigma_n) + K\Phi\left(\frac{\theta_m - \theta_{ext}}{\sigma_{ext}}\right) \quad (3)$$

$$w_{n\to m} = exp\left(\frac{-|\theta_n - \theta_m|^2}{2\sigma_w^2}\right) \quad (4)$$

The external input is a time-constant Gaussian curve peaked at target direction θ_{ext} (Eq. 3, Fig. 1F). Here, K is the scale factor, and σ_{ext}^2 represents the variance, hence determining the **external uncertainty**.

Simulating Decision Making. We examined the critical bifurcation phenomenon, where the output direction switched from average direction to align with one of the targets. The critical angle is identified as the smallest separation angle that causes this shift in all the simulated trajectories (N=100).

We simulated the network activity under each combination of internal noise and external uncertainty. We varied internal noise in the range [.1, 5] and external [1, 37]. These simulations were conducted at varying target separation angles θ (Fig. 2A), with the output direction updated at 1 ms intervals.

Results

We found critical bifurcation angle in the simulated trajectories (Fig. 2B). There exists a critical angle beyond which the network's output aligns with the direction of one of the targets, (Fig. 2D). This dynamics contrasts with conditions below the critical angle, where the network's output tends to represent an average direction between the two targets (Fig. 2C).

The critical angle is influenced by the levels of internal noise and external uncertainty within the system. Our result indicates that the critical angle increases with higher levels of in-

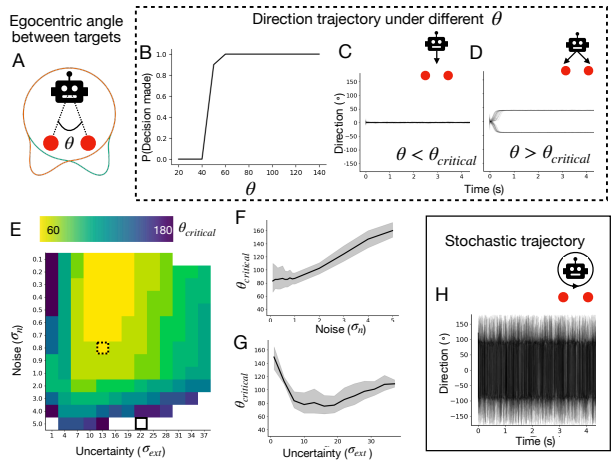

Figure 2: Results. **A)** Egocentric separation angle θ between targets (red dots). The orange and green curve denotes inputs to the ring attractor model. **B-D)** Direction trajectories at different separation angle θ when $\sigma_n = 0.8$ and $\sigma_{ext} = 13$. **B)** Proportion of trajectories aligned to a target direction increases dramatically around crtical angle. **C)** When θ was less than $\theta_{critical}$, simulated trajectories consistently align with the average direction between the two targets. **D)** when θ was bigger than $\theta_{critical}$, each simulated trajectory converge to one of the target directions arbitrarily. **E)** Maps the critical critical angle across varying levels of external noise and internal noise. Trajectories reflecting these bifurcations are presented in Panels B-D. White spots highlight conditions leading to unstable bifurcation in Panel H. **F)** The critical bifurcation angle increases with internal noise **G)** The bifurcation angle decreases and increases with external uncertainty. **H)** Chaotic condition ($\sigma_n = 5.0, \sigma_{ext} = 22$) where trajectory bifurcation remains unstable and cannot settle on a consistent direction.

ternal noise (Fig. 2F). However, when both external uncertainty and internal noise are minimal, the critical angle is maximized (Fig. 2E). External uncertainty modulates critical angle in a U-shape manner, when uncertainty increases, the bifurcation angle initially decreases and then increases (Fig. 2G).

Additionally, under certain combinations of internal noise and external uncertainty, the network exhibits stochastic dynamics, as shown in white space in (Fig. 2E). In these scenarios, the output direction fluctuates unpredictably between the two target directions without stabilizing on either (Fig. 2H).

Conclusion

We investigated how external uncertainty and internal noise would influence crtical bifurcation in spatial decision-making. The findings indicate that increased internal noise slows down the decision-making process and extends the travel distance required to reach the critical phase. Interestingly, both minimal and substantial levels of external uncertainty had similar effects. This modulation on the critical phase in dynamics provides new perspectives into SAT in spatial decision-making.

Acknowledgements

V.H.S. acknowledges support from the 'Collaborative Research Grant' funded jointly by the Department for the Ecology of Animal Societies, MPI-AB and the 'Center for the Advanced Study of Collective Behaviour' at the University of Konstanz, Deutsche Forschungsgemeinschaft Centre of Excellence 2117 (ID: 422037984). Y.X. acknowledges the financial support of 'International Max Planck Research School (IMPRS) for The Mechanisms of Mental Function and Dysfunction' (MMFD).

References

Agarap, A. F. (2019, February). *Deep Learning using Rectified Linear Units (ReLU)* (No. arXiv:1803.08375). arXiv. doi: 10.48550/arXiv.1803.08375

Amil, A. F., & Verschure, P. F. M. J. (2021, December). Supercritical dynamics at the edge-of-chaos underlies optimal decision-making. *Journal of Physics: Complexity*, *2*(4), 045017. doi: 10.1088/2632-072X/ac3ad2

Bertucco, M., Bhanpuri, N. H., & Sanger, T. D. (2015, October). Perceived Cost and Intrinsic Motor Variability Modulate the Speed-Accuracy Trade-Off. *PLOS ONE*, *10*(10), e0139988. doi: 10.1371/journal.pone.0139988

Brette, R., & Gerstner, W. (2005, November). Adaptive Exponential Integrate-and-Fire Model as an Effective Description of Neuronal Activity. *Journal of Neurophysiology*, *94*(5), 3637–3642. doi: 10.1152/jn.00686.2005

Cocchi, L., Gollo, L. L., Zalesky, A., & Breakspear, M. (2017, November). Criticality in the brain: A synthesis of neurobiology, models and cognition. *Progress in Neurobiology*, *158*, 132–152. doi: 10.1016/j.pneurobio.2017.07.002

Hulse, B. K., & Jayaraman, V. (2020). Mechanisms Underlying the Neural Computation of Head Direction. *Annual Review of Neuroscience*, *43*(1), 31–54. doi: 10.1146/annurev-neuro-072116-031516

Kutschireiter, A., Basnak, M. A., Wilson, R. I., & Drugowitsch, J. (2023, February). Bayesian inference in ring attractor networks. *Proceedings of the National Academy of Sciences*, *120*(9), e2210622120. doi: 10.1073/pnas.2210622120

Manohar, S. G., Chong, T. T.-J., Apps, M. A., Batla, A., Stamelou, M., Jarman, P. R., ... Husain, M. (2015, June). Reward Pays the Cost of Noise Reduction in Motor and Cognitive Control. *Current Biology*, *25*(13), 1707–1716. doi: 10.1016/j.cub.2015.05.038

Mendonça, A. G., Drugowitsch, J., Vicente, M. I., DeWitt, E. E. J., Pouget, A., & Mainen, Z. F. (2020, June). The impact of learning on perceptual decisions and its implication for speed-accuracy tradeoffs. *Nature Communications*, *11*(1), 2757. doi: 10.1038/s41467-020-16196-7

Sridhar, V. H., Li, L., Gorbonos, D., Nagy, M., Schell, B. R., Sorochkin, T., ... Couzin, I. D. (2021, December). The geometry of decision-making in individuals and collectives. *Proceedings of the National Academy of Sciences*, *118*(50), e2102157118. doi: 10.1073/pnas.2102157118

Sun, X., Mangan, M., & Yue, S. (2018). An Analysis of a Ring Attractor Model for Cue Integration. In V. Vouloutsi et al. (Eds.), *Biomimetic and Biohybrid Systems* (Vol. 10928, pp. 459–470). Cham: Springer International Publishing. doi: 10.1007/978-3-319-95972-6_49

Touretzky, D. S. (2005, July). Attractor Network Models of Head Direction Cells. In S. I. Wiener & J. S. Taube (Eds.), *Head Direction Cells and the Neural Mechanisms of Spatial Orientation* (pp. 411–432). The MIT Press. doi: 10.7551/mitpress/3447.003.0026

Wang, C., & Zhang, K. (2020). Equilibrium States and Their Stability in the Head-Direction Ring Network. *Frontiers in Computational Neuroscience*, *13*.

Wilson, R. I. (2023). Neural Networks for Navigation: From Connections to Computations. *Annual Review of Neuroscience*, *46*(1), 403–423. doi: 10.1146/annurev-neuro-110920-032645